ELSEVIER

Contents lists available at ScienceDirect

Marine Pollution Bulletin

journal homepage: www.elsevier.com/locate/marpolbul





Modeling impacts of river hydrodynamics on fate and transport of microplastics in riverine environments

Xiaolong Geng ^{a,b}, Michel C. Boufadel ^{c,*}, Edward P. Lopez ^a

- ^a Department of Earth Sciences, University of Hawai'i at Manoa, Honolulu, HI 96822, USA
- ^b Water Resources Research Center, University of Hawai'i at Mānoa, Honolulu, HI 96822, USA
- ^c Department of Civil and Environmental Engineering, New Jersey Institute of Technology, University Heights, Newark, NJ 07102, USA

ARTICLE INFO

Keywords: Microplastics River hydrodynamics Aggregation and breakage OpenFOAM Numerical modeling

ABSTRACT

Microplastics pose a significant and growing threat to marine ecosystems and human health. Rivers serve as critical pathways for the entry of inland-produced microplastics into marine environments. In this paper, we developed a numerical modeling scheme using OpenFOAM to investigate the fate and transport of microplastics in a river system. Our simulation results show that microplastics undergo significant aggregation and breakage as they are transported downstream by river flows. This significantly alters the particle size distribution of microplastics. The aggregation-breakage process is mainly controlled by river hydrodynamics and pollution scale. Our findings suggest that a significant extent of particle aggregation occurs at an early stage of the release of microplastics in the river, while the aggregation-breakage process becomes limited as the microplastic plume is gradually dispersed and diluted downstream. Eddy diffusivity drives the dispersion of the microplastic plume in the river, and its spatial patterns affect the aggregation-breakage process.

1. Introduction

Annual plastic production worldwide increased exponentially from 2 million tons in 1950 to 391 million in 2021 (PlasticsEurope, 2021). Such wide uses of plastic products have been considered as one of the primary environmental problems negatively affecting marine ecosystems across the world. Studies indicate that over 250 marine species are believed to be contaminated by plastic ingestion (Anbumani and Kakkar, 2018; Laist, 1997). The plastic debris present in rivers, estuaries, and oceans is often subjected to fragmentation over time, as a result of photooxidation, the action of wind, current, and waves, and biodegradation (Auta et al., 2017; Borges-Ramírez et al., 2020). The plastic particles, size <5 mm, are usually defined as microplastics. Among plastic debris of different sizes, microplastics have been found to be ubiquitously present and persist for a long duration in marine ecosystems (NOAA, 2016; Williams and Simmons, 1996). Microplastics are of special concern as 'emerging contaminants', since their small size facilitates internalization by biota and adsorption of pollutants on their surface (Deng et al., 2017; Koelmans et al., 2016; Rillig, 2012; Schirinzi et al., 2017). Therefore, studies on the abundance, distribution, and fate of microplastics are becoming crucial to evaluate their stress on terrestrial and aquatic ecosystems (Lenaker et al., 2020; Pan et al., 2019; Tibbetts et al., 2018).

Marine microplastic pollution is mainly derived from terrestrial sources, such as domestic, commercial, and industrial wastewater, stormwater runoff, and effluents and sludges from wastewater treatment plants (Dris et al., 2017; Dris et al., 2015). Rivers have been recognized as important pathways for the transport and fate of microplastics into the ocean (Mani et al., 2015; McCormick et al., 2016; Tibbetts et al., 2018). Lebreton et al. (2017) presented a global model of plastic inputs from rivers into oceans based on waste management, population density, and hydrological information. Their model estimated that between 1.15 and 2.41 million tonnes of plastic waste currently enter the ocean every year from rivers, with over 74 % of releases occurring between May and October. The top 20 polluting rivers, mostly located in Asia, account for 67 % of the global total. Moore et al. (2005) measured that as high as ~1.3 billion plastic particles per day flowed into the Pacific Ocean from 2 rivers in Southern California, USA. Yonkos et al. (2014) collected surface water samples to enumerate microplastics from four estuarine tributaries within the Chesapeake Bay, New Jersey, USA. Their measurements show that the microplastic concentration in the Chesapeake Bay varied from ~5500 particles/km² to ~300,000 particles/ km², which demonstrated positive correlations with population density and proportion of urban/suburban development within watersheds. Sutton et al. (2016) present the information on abundance, distribution,

E-mail address: boufadel@gmail.com (M.C. Boufadel).

 $^{^{\}ast}$ Corresponding author.

and composition of microplastics at nine sites in San Francisco Bay, California, USA. They found that with an average microplastic abundance of ~700,000 particles/km2, the surface water appears to have higher microplastic levels than other urban water bodies sampled in North America. van der Wal et al. (2015) estimated the riverine plastic loads to European regional seas. The measurements indicate that the annual loads of microplastics (particles/year) from the Danube River to the Black Sea, from Po River to the Mediterranean Sea, and from the Rhine River to the North Sea are 2 trillion, 0.7 trillion, and 0.4 trillion, respectively. Eo et al. (2019) measured the abundance of microplastics in the Nakdong River and estimated the annual load of microplastics carried by the river in 2017 to be 5.4-11 trillion by number. Mai et al. (2019) conducted sampling at the eight major river outlets of the Pearl River Delta (PRD), South China, and estimated the annual riverine input of microplastics from the PRD into the South China sea was estimated to be 39 billion particles.

The fate and transport of microplastics in rivers are driven by several fundamental processes. By means of riverine hydrodynamic forces and particle properties (e.g., size, density, and fractal dimension), microplastics usually undergo advection, dispersion, suspension, and settling in the water column (Atugoda et al., 2020). Advection refers to the streamwise transport following river flow velocity. Dispersion often represents mass transfer driven by shear flow coupled to a concentration gradient (i.e., spreading of mass from high concentration region to low concentration region). Besides being transported in the river, particles with a different density than the surrounding will have a vertical motion due to buoyancy, they can remain at the water surface (Cui et al., 2021a) or sink and deposit onto the sediments (Cui et al., 2021b; Khatmullina and Isachenko, 2017; Waldschläger and Schüttrumpf, 2019), and may reenter the water column attributed to erosion/resuspension of the riverbed (Hurley et al., 2018; Yan et al., 2021). During transport in riverine systems, microplastics may also be subjected to aggregation and breakage. Aggregation involves the motion of two particles toward each other to collide, followed by attachment. It can occur with two particles of the same type (called homoaggregation), or two different particles (called heteroaggregation) such as aggregation between microplastics and clay minerals and/or biota (Alimi et al., 2018). The aggregation of particles is usually conceptualized using the von Smoluchowski model. In the model, the formation of aggregates is kinetically formulated as a function of the colliding particle concentration, their size and densities, their collision frequencies and efficiencies (Barton et al., 2014; Ji et al., 2021; Kooi et al., 2018; Liu et al., 2023; Zhao et al., 2016a; Zhao et al., 2014). Following the population balance equation, Zhao et al. (2014) developed a comprehensive numerical model, VDROP, to simulate the transient oil droplet size distribution in turbulent regimes, which has been substantially used in the studies on the formation of droplets in aquatic environments (Cao et al., 2021; Liu et al., 2022; Ye et al., 2020; Zhao et al., 2017). Cui et al. (2021a) developed a numerical frame that coupled the VDROP model with river hydrodynamics to investigate the dispersion of oil droplets in riverine systems. The study revealed a significant breakup of oil droplets in rivers driven by the high energy dissipation rate in the water column. Ji et al. (2021) conducted lab experiments to investigate the impact of mixing energy on the formation of oil-particle aggregates. In particular, their study revealed that at high mixing energy, turbulent mixing dominates particle collision frequency.

Numerical modeling has been recognized as an important tool in predicting the fate and transport of microplastics in aquatic systems (Wagner and Lambert, 2018). The modeling approach could mainly fall into two categories: Lagrangian particle tracking algorithms that deal with individual particles and track the trajectory of individual particles separately, and Eulerian models that describe particles in terms of their mass or volume concentrations. Previous numerical studies have demonstrated that the distribution of microplastics in the ocean can be predicted using Lagrangian tracking models, taking into account current, wind, and horizontal diffusion (Eriksen et al., 2013; Law and Thompson, 2014; Lebreton et al., 2012; Potemra, 2012; Zhang et al.,

2020). For instance, Lebreton et al. (2012) used the Lagrangian particle tracking model Pol3DD to simulate the floating debris in the world's oceans and simulated the high concentration in subtropical gyres. Zhang et al. (2020) implemented a Lagrangian particle tracking model to investigate the dispersion of suspended and floating microplastic particles in the East China Sea and adjacent seas. Their results identified three major delivery channels for microplastics released from the coastal areas of China, Korea, and Japan. The Eulerian formulation has also been widely used for predicting the transport and distribution of microplastics. Mountford and Morales Maqueda (2019) used an Eulerian model based on the 3-D global ocean model Nucleus for European Modelling of the Ocean (NEMO) to simulate the dispersion of plastics in the global ocean. Their modeling results support the observation of positively buoyant plastic accumulations in the five garbage patches within subtropical ocean gyres; by contrast, the negatively buoyant plastic tends to accumulate within the deepest regions of the sea floor, loosely following the bathymetry. Genc et al. (2020) used the Eulerian scheme to simulate the advection and diffusion of 3 mm size polystyrene particles by the coastal currents in the surface waters of Fethive Inner Bay, Turkey. Their simulation results revealed that microplastic accumulation is expected in certain regions of the bay.

Although considerable efforts were made to simulate the fate and transport of microplastics, numerical studies on plastic migration in riverine systems are scarce. Inspired by an existing global model for nutrients, Siegfried et al. (2017) adopted the Global NEWS model to calculate river export of microplastics from point sources as a function of human activities on land and river retention. Their model was implemented at a relatively large scale, based on the STN-30p river system (Vörösmarty et al., 2000) at a grid of $0.5^{\circ} \times 0.5^{\circ}$. However, a sophisticated numerical scheme integrating various physical processes that regulate the fate and transport of microplastics has not yet been developed-a research gap this paper aims to address.

The objective of this paper is to investigate the fate and transport of microplastics in river systems, considering advection, dispersion, suspension, settling, aggregation, and breakage processes. A numerical model was developed to simulate the fate and transport of microplastics in a river system. The model coupled river hydrodynamics and particle aggregation-breakage kinetics to multiple interactive transport equations, each of which corresponds to microplastics within a particular size range. Impacts of the aggregation-breakage process as well as spatial variation of diffusivity on the fate and transport of microplastics in the river system were quantified. The paper provides insights into better understanding the fate and transport of microplastics in riverine systems.

2. Methodology

2.1. River hydrodynamics

The vertical velocity profile u(z) can be expressed as a function of water elevation above streambed (z) by the log-wake formulation (Boufadel et al., 2018; Nezu and Nakagawa, 1993; White, 1991):

$$\frac{u_x(z)}{u^*} = \frac{1}{\kappa} ln \left(\frac{z}{k_s}\right) + w + \chi. \tag{1}$$

where $\kappa=0.41$ is the Von Karman constant; $k_{\rm s}=$ riverbed roughness height; and χ is an empirical constant. Nezu et al. (1994) have suggested $\chi=8.5$ for completely rough beds, which will be used in this paper. For a stream with constant water depth, the friction velocity u_* can be estimated by Boufadel et al. (2019):

$$u_* = \sqrt{gR_hS}. (2)$$

where S = slope of the river; g = acceleration of gravity; and R_h = hydraulic radius. The second term on the right side of Eq. (1) is the wake function, defined as (Coles, 1956)

$$w(z) = \frac{2\prod_{\kappa} \sin^2\left(\frac{\pi z}{2h}\right)}{\ln L}.$$
 (3)

where h = water depth; and Π is the wake strength parameter.

To account for the effect of the roughness at the boundary, we derived the eddy viscosity profile (i.e., eddy diffusivity profile) by introducing roughness heights at the surface and bottom of the river, expressed as follows:

$$\frac{\nu_{t}(z)}{u_{*}} = \kappa \left[z + z_{b} \left(1 - \frac{z}{h} \right) \right] \left(1 - \frac{z}{h} + z_{s} \frac{z}{h^{2}} \right). \tag{4}$$

where z_b and z_s represent roughness height at the river bottom and surface, respectively. Herein, we assumed $z_b \approx 0.1k_s$, and $z_s \approx 0.1k_s$. This is an approach that we adopted in our prior work (Boufadel et al., 2020). The parameter k_s denotes the bottom roughness height, which can be estimated from the following expression (Limerinos, 1970).

$$\frac{n}{R_h^{1/6}} = \frac{1}{21.9log12.2\frac{R_h}{L}} \tag{5}$$

where n denotes the Manning roughness coefficient.

An important parameter determining the breakup of aggregated particles in a turbulent regime is the energy dissipation rate, ε (Hinze, 1955; Zhao et al., 2014). Techniques for estimating or measuring it have been conducted in oceanic (Terray et al., 1996) and laboratory (Kaku et al., 2006; Zhao et al., 2016b) systems. In river systems, Nezu (2005) proposed a universal function based on the experimental data of Nezu (1977) using hot film anemometry and of Komori et al. (1989) using laser Doppler anemometry. The expression for ε is

$$\frac{\varepsilon h}{u_*^3} = 9.8 \left(\frac{z}{h}\right)^{-1/2} \left[exp\left(-3\frac{z}{h}\right) \right]. \tag{6}$$

2.2. Aggregation and breakage kinetics

The aggregation-breakage dynamics of microplastics can be formalized by the change in particle-size distribution attributed to particle aggregation and aggregate breakage. Such kinetics has been expressed below, following the form of the Smoluchowski equation (Coufort et al., 2007; Flesch et al., 1999; Shi et al., 2019; Smoluchowski, 1918; Zhang and Li, 2003):

$$\frac{dn(m)}{dt} = \frac{1}{2} \int_0^m \alpha \beta n(m-x) n(x) dx - \int_0^\infty \alpha \beta n(m) n(x) dx - sn(m) + \int_m^\infty \gamma sn(x) dx.$$
(7)

where t is time; n(m) is the particle size distribution with respect to the size identified by mass m; α represents the collision efficiency; β represents the collision frequency; s represents the breakup rate of the aggregates; γ represents the breakage distribution function that defines the mass fraction of the fragments of size m breaking from the larger size aggregates. Here we assumed binary breakage, which defines the breakup of an aggregate into two equal fragments. On the right-hand side of Eq. (7), the first term is the gain term for the particle of size m attributed to aggregation between smaller particles; the second term represents the loss of aggregates of size m due to the increase in size by aggregation with other particles; the third term is for the loss of the aggregates of size m due to their breakage, and the fourth term represents the gain of aggregates of size m from the breakage of larger size aggregates.

2.3. Sectional governing equations

The sectional approach has been widely used to solve Eq. (7) (Gelbard et al., 1980; Hounslow, 1998). Following the common practice, the generation of size sections follows the rule that the upper bound of a section is twice its lower bound in terms of particle mass (i.e., m_k =

 $2m_{k-1}$). Within a given section (e.g., the kth section), there are seven scenarios of aggregation and breakage that result in the gain and loss of particle mass, and the sectional governing equations can be expressed as follows:

$$\frac{dM_k}{dt} = A \sum_{i=1}^{k-1} \int_{m_{i-1}}^{m_i} \int_{m_{k-1}-x}^{m_{k-1}} \alpha \beta n(x) n(y)(x+y) dy dx$$

$$+ \sum_{i=1}^{k-1} \int_{m_{i-1}}^{m_i} \int_{m_{k-1}}^{m_k-x} \alpha \beta n(x) n(y) x dy dx - \sum_{i=1}^{k} \int_{m_{i-1}}^{m_i} \int_{m_{k-1}}^{m_k} \alpha \beta n(x) n(y) y dy dx$$

$$- \frac{1}{2} \int_{m_{k-1}}^{m_k} \int_{m_{k-1}}^{m_k} \alpha \beta n(x) n(y)(x+y) dy dx - \sum_{i=k+1}^{N} \int_{m_{k-1}}^{m_k} \int_{m_{i-1}}^{m_i} \alpha \beta n(x) n(y) y dy dx$$

$$- \int_{m_{k-1}}^{m_k} s n(x) x dx dy + \sum_{i=k+1}^{N} \int_{m_{k-1}}^{m_k} \int_{m_{i-1}}^{m_i} \gamma s n(y) y dy dx.$$

$$(8)$$

where N denotes the total number of sections; M_k denotes the total mass concentration within the kth section. Since $M_i = \int_{m_{i-1}}^{m_i} x n(x) dx$ (Seinfeld and Pandis, 2008), on the right-hand side of Eq. (8) the particle size distribution within the ith section $n(x) = \frac{M_i}{(\ln 2)x^2}$; coefficient $A = \{0.5, i = k-1; 1.0, i < k-1\}$. The seven particle interaction terms at the right-hand side are described in detail in Fig. 1.

2.4. Collision frequency and breakup rate

The collision frequency β is based on the collision mechanism between entities of different sizes due to turbulent shear, differential settling, and Brownian motion. For spherical entities, these three mechanisms are given by prior studies (Cui et al., 2021b; Ernest et al., 1995; Jiang and Logan, 1991; Zhao et al., 2016a):

For turbulent shear

$$\beta_{sh}(i,j) = \frac{1}{6} \left(\frac{\varepsilon}{\nu_w} \right)^{1/2} \left(d_i + d_j \right)^3 \tag{9}$$

For differential settling

$$\beta_{ds}(i,j) = \frac{\pi}{4} (d_i + d_j)^2 |w_i - w_j|$$
 (10)

For Brownian motion

$$\beta_{Br}(i,j) = \frac{2\kappa T}{3\rho_{\omega}\nu} \left(\frac{1}{d_i} + \frac{1}{d_i}\right) \left(d_i + d_j\right) \tag{11}$$

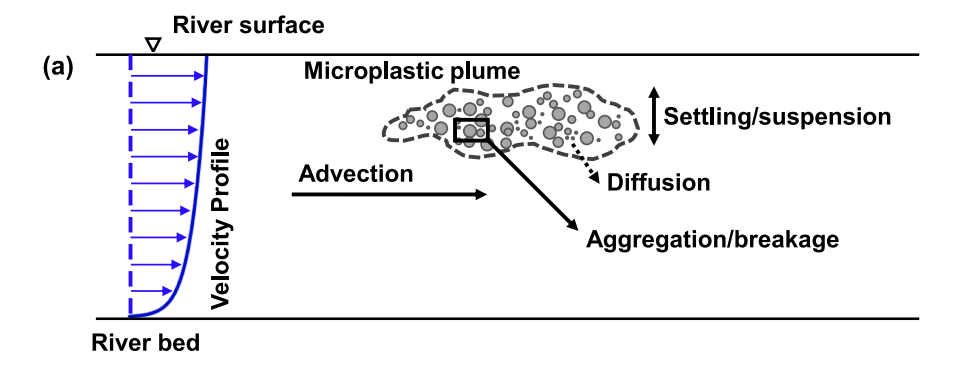
The three interparticle collision frequency functions are independent and additive, and thereby,

$$\beta(i,j) = \beta_{sh}(i,j) + \beta_{ds}(i,j) + \beta_{Br}(i,j).$$
 (12)

where d_i and d_j represent the equivalent diameter of two colliding entities, respectively; v_w and μ represents the kinematic and dynamic of water, respectively; ρ_w represents the density of water; κ is the Boltzmann constant equal to 1.38×10^{-23} (J/K); w_i and w_j represent the slip velocity (i.e., due to buoyancy), which can be obtained as follows (Zhao et al., 2015)

$$w = \frac{g(\rho_p - \rho_w)m}{3\pi\mu\rho_c d} \tag{13}$$

Eq. (13) implies that larger particle size leads to higher slip velocity. Such an effect is considered in the simulation by incorporating Eq. (13) to the transport equations of microplastics expressed in Eq. (15). The breakage rate can be formalized as a function of the shear rate (i.e.,



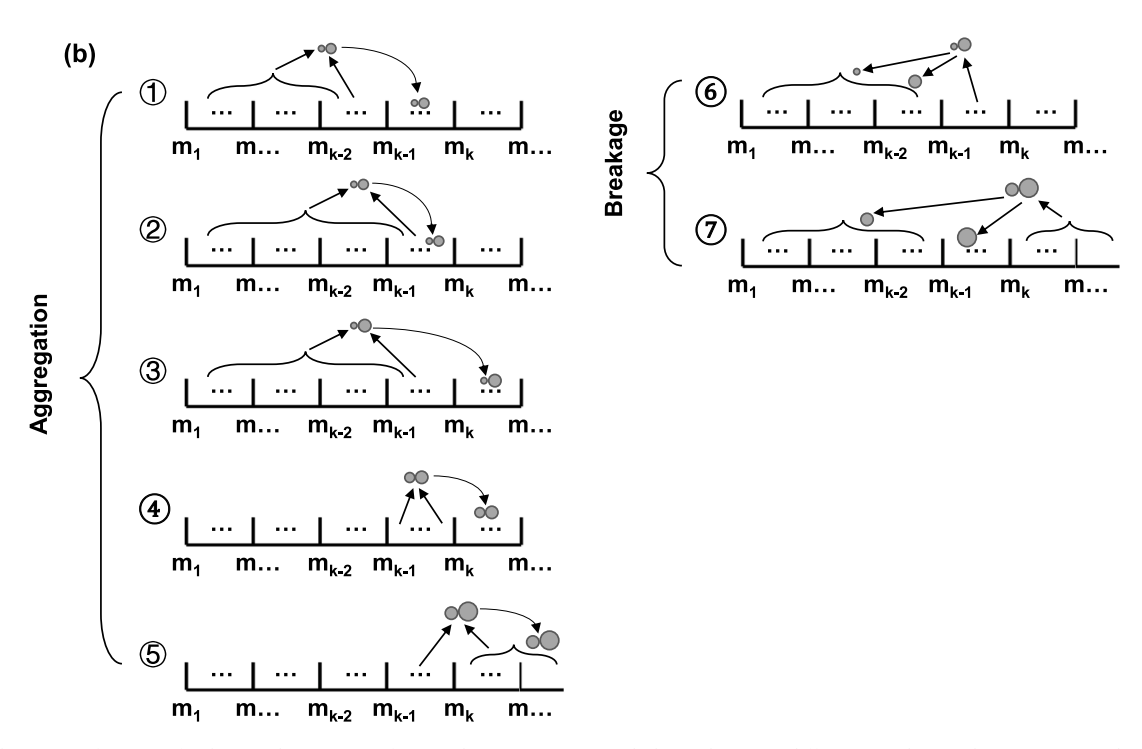


Fig. 1. (a) Schematics of various fundamental processes of microplastics in rivers, including advection, diffusion, settling and suspension, and aggregation and breakage; (b) seven scenarios of particle aggregation (1–5) and breakage (6–7) within the sectional approach. Note that the microplastic plume is delineated with a dashed closed curve, within which spheres represent microplastics of varying particle sizes. The seven scenarios of particle aggregation and breakage correspond to the seven integration terms on the right-hand side of Eq. (8).

 $\left(\frac{e}{\nu_w}\right)^{1/2}$), and the aggregate volume (i.e., $\frac{m}{\rho_p}$) (Chen et al., 1990; Flesch et al., 1999; Peng and Williams, 1994)

$$s = E \left(\frac{\varepsilon}{\nu_w}\right)^{b/2} \left(\frac{m}{\rho_p}\right)^{1/3} \tag{14}$$

where *E* and *b* are the breakage rate constants, which have been estimated to be 7×10^{-4} and 1.6, respectively, in Flesch et al. (1999).

2.5. Transport of microplastics

The movement of dispersed entities is simulated as passive scalars by the advection-diffusion-reaction equations, given by.

$$\frac{\partial M_k}{\partial t} = \nabla \cdot \left(\overrightarrow{D} \nabla M_k \right) - \nabla \cdot (\overrightarrow{u} M_k) + r_k, \qquad k = 1, 2, ..., N$$
 (15)

where the eddy diffusivity \overrightarrow{D} is assumed isotropic and calculated by Eq. (4), and the velocity vector $\overrightarrow{u} = (u_x, w_k)$; the source term r_k represents the aggregation-breakage processes of microplastics within the kth

section, described by Eq. (8). Note that the advection-diffusion-reaction model has been substantially used in our prior studies for various applications (e.g., Cui et al., 2021a; Cui et al., 2021b; Geng et al., 2017; Geng et al., 2015; Geng et al., 2016).

2.6. Numerical implementation

The simulations were conducted through the OpenFOAM platform using the scalarTransporFoam solver. The scenario simulated herein is a point-source release of microplastics into a river channel. The width of the river is considered infinite, and therefore, the approach focuses on a vertical profile away from the river banks. The river water depth was assumed to be 4 m with a very mild slope of 1.5×10^{-5} , and the resulting mean velocity is 0.3 m/s. Such an assumption was based loosely on a river system at the Lower Passaic River, New Jersey (Wilson and homologs Dec, 2006). In river systems, microplastics denser than water do not readily reach distant regions, as they sink through the water column due to their high density. Therefore, microplastics lighter than water were selected for this numerical investigation. The primary microplastics were assumed 2.0 μ m in diameter with a density of 900 kg/m³.

As we considered microplastics with density less than water, the settling process of microplastics was automatically excluded in the simulation. Here, 27 contiguous-size sections, labeled c1-c27, were considered with the setting of $m_k=2m_{k-1}$, leading to a range of diameter from 2.0 µm to ~500 µm. For instance, the first six size bins are listed as follows: [2 µm, 2.52 µm], [2.52 µm, 3.17 µm], [3.17 µm, 4.0 µm], [2 µm, 5.04 µm], [5.04 µm, 6.35 µm], and [6.35 µm, 8 µm]. The aggregation-breakage model written in C++ was built up as an independent module into the OpenFOAM platform, coupled with ScalarTransportFoam at every time step.

To validate the functionality of the aggregation-breakage model, we first conducted simulations without transport to reproduce the aggregation-breakage results presented in Zhang and Li (2003) and Li and Zhang (2003). In their study, the particle aggregation-breakage process was simulated under two different conditions with the initial concentration of the primary particles (Q_0), shear rate ($\left(\frac{\varepsilon}{\nu_w}\right)^{1/2}$), and fractal dimension (D) equal to 5.0×10^{-5} kg/m³, 50 s⁻¹, and 2.5, and 5.0×10^{-3} kg/m³, 15 s⁻¹, and 3.0, in Zhang and Li (2003) and Li and Zhang (2003), respectively. The primary particles were 1 µm in diameter with a density of 1.2 g·cm⁻². The whole size range was from 1 µm to approximately 1 cm for particles, which extended further for fractal particle aggregates. There were 42 contiguous-size sections with the setting of $m_k = 2m_{k-1}$ for the lower and upper bounds of the k_{th} section.

To simulate the fate and transport of microplastics in rivers, the implementation is described as follows. The size of the domain was 200 m (L) \times 5 m (H). The domain was first discretized with a grid resolution of 2 cm and then refined with a vertical resolution of \sim 5 mm in the proximity of the river surface between 3.5 m and 4.2 m, resulting in ~600,000 computational cells. The primary particles were instantaneously released as a point source ~10 cm below the river surface and 10 m away from the inlet boundary with a mass concentration of 5.0 kg/ m³. Note that the high initial mass concentration was adopted for the simulations to enable a more comprehensive analysis of how the particle size distribution evolves over a wide range of microplastic mass concentrations, especially as the microplastic plume becomes diluted during downstream transport by river flows. The streamwise periodic boundary conditions, a so-called cyclic (translational) boundary in the Open-FOAM, were implemented at the inlet and outlet boundaries. The periodic boundary condition defines a physical connection between the outlet and inlet boundaries, creating a cyclic situation of the flow and solute across the boundaries. Such configuration could allow the simulation of the flow and transport processes in an infinitely long river channel using a smaller-length domain. No-flux boundary conditions were implemented at the river surface and riverbed.

Simulations conducted in this study include the transport of microplastics with and without aggregation-breakup processes. Prior studies identified the impacts of eddy diffusivity on transport processes in aquatic systems (e.g., Boufadel et al., 2020; López and García, 1998). Therefore, simulations were conducted with spatially varied and constant diffusivities, respectively. The constant diffusivity is set as the integrated average of the spatially varied diffusivity along its vertical profile (Eq. (4)), as done by Boufadel et al. (2020). The simulations aim to reveal the effects of particle aggregation and breakage on the fate and transport of microplastics in river systems. In addition, different diffusivity profiles were adopted in the simulations to further quantify the impacts of spatial variation in eddy diffusivity on simulating the fate and transport of microplastics in river environments.

3. Results

The characteristics of the river hydrodynamics in the OpenFOAM simulations are delineated in Fig. 2. The streamwise velocity was nearly zero at the riverbed due to bottom friction, and it increased with elevation by reaching the maximum of 0.4 m/s near the river surface (Fig. 2a). The increase in river velocity with elevation followed the

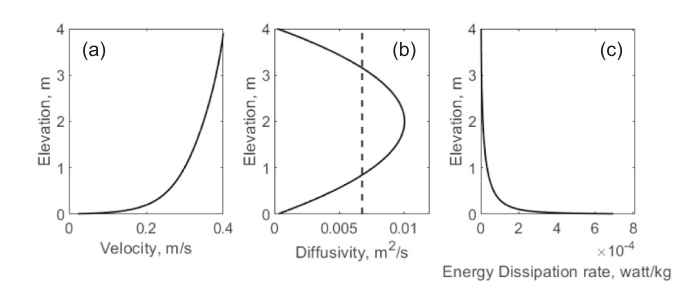


Fig. 2. River hydrodynamics of (a) streamwise velocity, (b) eddy diffusivity, and (c) energy dissipation rate. Note that the dashed line in panel b denotes the integrated average of the eddy diffusivity along its vertical profile, which is used in the simulations with constant diffusivity.

logarithmic growth where the velocity gradients were the largest near the riverbed and tended to be smaller as elevation increased. The eddy diffusivity exhibited small values adjacent to the river surface and bottom, which is equal to 10 % of the bottom roughness height, illustrated in Eq. (1), while below the river surface and above the river bed, the diffusivity gradually increased and reached a maximum value of $\sim\!0.01$ m²/s at the mid-elevation of 2.0 m above the riverbed (Fig. 2b). The average of the eddy diffusivity of 6.68 \times 10 $^{-3}$ m²/s was adopted in the cases simulated with a constant eddy diffusivity. The energy dissipation rate (\$\epsilon\$) could have strong impacts on the aggregation and breakage of microplastics, and therefore its vertical profile is shown in Fig. 2c, demonstrating that \$\epsilon\$ was the lowest at the river surface and increased with depth by reaching the maximum of $\sim\!\!7\times10^{-4}$ watt/kg near the riverbed

Fig. 3 shows the temporal evolution of particle size distribution caused by aggregation and breakage under different mixing conditions. The results demonstrate that the simulations conducted in this paper well reproduced the evolution of particle size distribution that was modeled in the prior studies of Zhang and Li (2003) and Li and Zhang (2003). In the early phase of the aggregation-breakage process, the particle size distribution gradually shifted to large-size bins with time, indicating significant aggregation of particles occurred. After major particle aggregation occurred, the particle size distributions tended to be stable. Specifically, in Fig. 3a, the particle size distribution reached a steady state after 15,000 s. Therefore, the distribution remained the same afterward. This is most likely because particle aggregates tended to be more fragile as their size increased, and the resulting breakage limited the continuous growth of particle sizes. Eventually, a steady state was reached as the rates of aggregation and breakage were nearly equal to each other, which ceased any significant changes in particle size distribution.

The microplastics experience significant aggregation as they moved downstream driven by river flows (Fig. 4). The simulation of the noreaction case shows that the point-source release of the microplastics in the river system generated a microplastic plume that migrated and expanded downstream with river flows, driven by advection and dispersion, respectively. The microplastic plume formed a remarkable tail as the plume migrated downstream and expanded to the river bed. This is most likely due to relatively low streamwise velocity caused by bottom friction, which limited the advection of microplastics near the river bed. By contrast, the simulation taking into account microplastics' aggregation and breakage process demonstrates a relatively low concentration of the microplastics within the smallest size bin (i.e., c1, the initial size of the microplastics), indicating significant aggregation of microplastics occurred in the river along with their downstream transport. This fact can also be proved by the concentration contour of microplastics within large-size bins (e.g., c2 and c3). Large-size aggregates are quickly generated after the release of the small-size microplastics in the river, which migrated and spread downstream. In particular, the contours show that the concentrations of microplastic

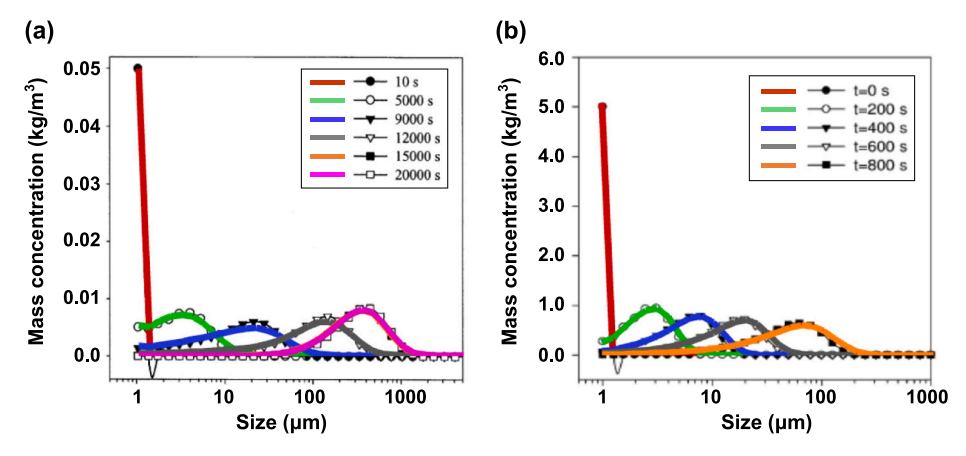


Fig. 3. Modeling results of the particle aggregation-breakage examples presented in Zhang and Li (2003) and Li and Zhang (2003). The results represent the evolution of particle size distribution at different time under a certain mixing condition. Note that bold-colored lines and symbolic lines represent the results simulated in this paper and Zhang and Li (2003) and Li and Zhang (2003), respectively. The unit of 's' marked in the legends denotes second. (For interpretation of the references to color in this figure legend, the reader is referred to the web version of this article.)

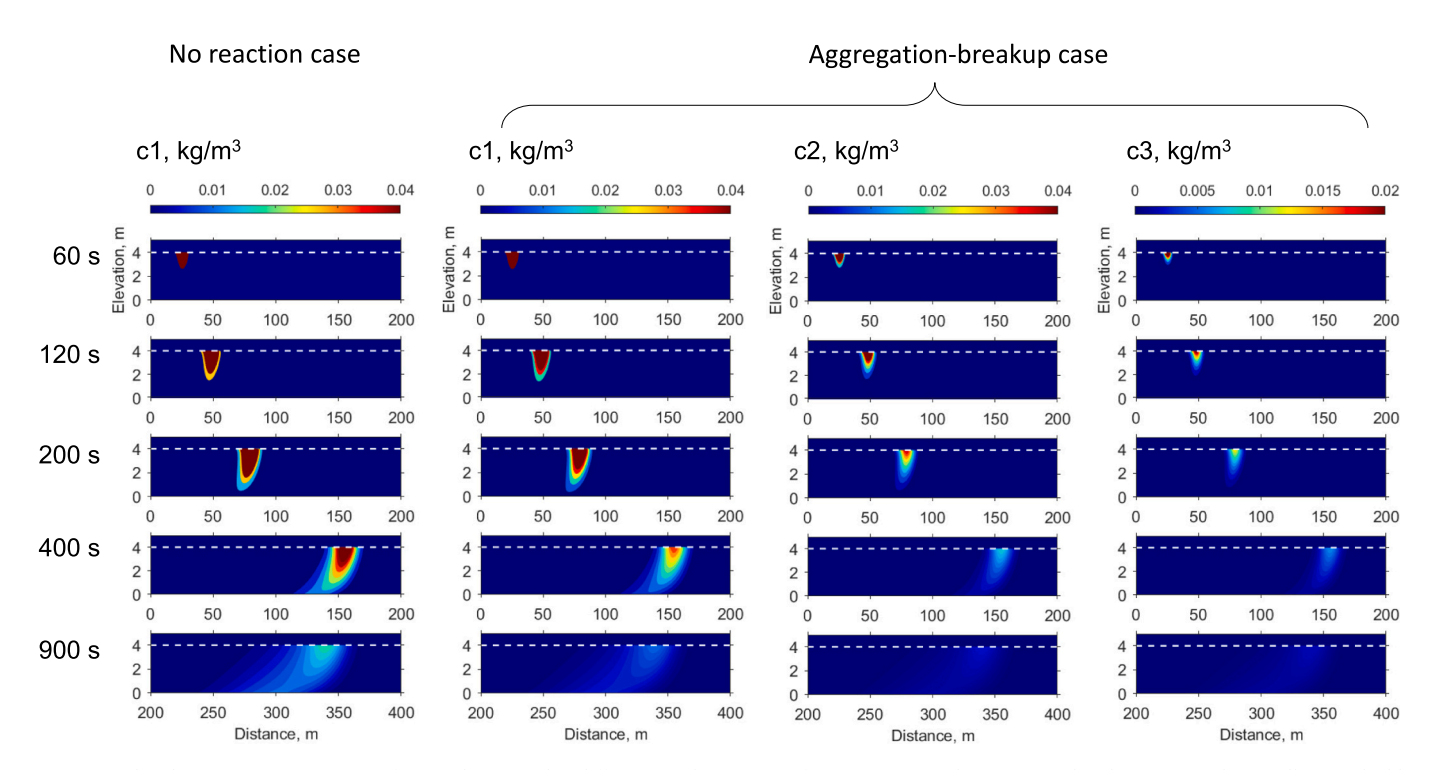


Fig. 4. Simulated concentration contours of microplastics within different size bins (c1–c3) for no reaction and aggregation-breakup cases with spatially varied eddy diffusivity. The c1, c2, and c3 represent the first three size bins, respectively.

plume within size bins c1 and c2 are in the same order of magnitude, indicating significant particle aggregation occurred in the river.

Spatial distributions of eddy diffusivity have strong impacts on the transport and aggregation of microplastics as they migrate downstream in a river system. When a spatially varied diffusivity was adopted, the vertical profile at the horizontal centroid of the microplastic plume show a higher concentration near the river surface and a lower concentration at a relatively lower elevation at the early stage of the transport (e.g., $t=100\,$ s and $500\,$ s), compared to the case simulated with the constant diffusivity (Fig. 5). It is consistent with the spatial distribution of eddy diffusivity along the river depth. For the case simulated with spatially varied diffusivity, extremely low diffusivity near the river surface limited dispersion of the microplastic plume there, while relatively higher diffusivity near the mid-depth of the river to some extent intensified microplastics to disperse at the deeper location. At a later stage (e.

g., t=900~s), it shows relatively high microplastic concentration along all the depths in the river for the case simulated with spatially varied diffusivity. This is because the microplastics simulated in this paper were lighter than water, and therefore they tended to float near the river surface. For the case simulated with spatially varied diffusivity, relatively low eddy diffusivity near the river surface to some extent limited overall dispersion of the microplastic plume in the river. As shown in the figure, such mechanisms applied to both aggregation-breakage and no reaction cases for all the simulated particle sizes. Fig. 5 also demonstrates significant aggregation of microplastics as they migrated downstream along with river flows. A remarkable amount of microplastics within size bins larger than c1 was formed (e.g., c2 and c3) with similar vertical distribution patterns, indicating an important interplay between the transport process and aggregation-breakage process of microplastics in the river.

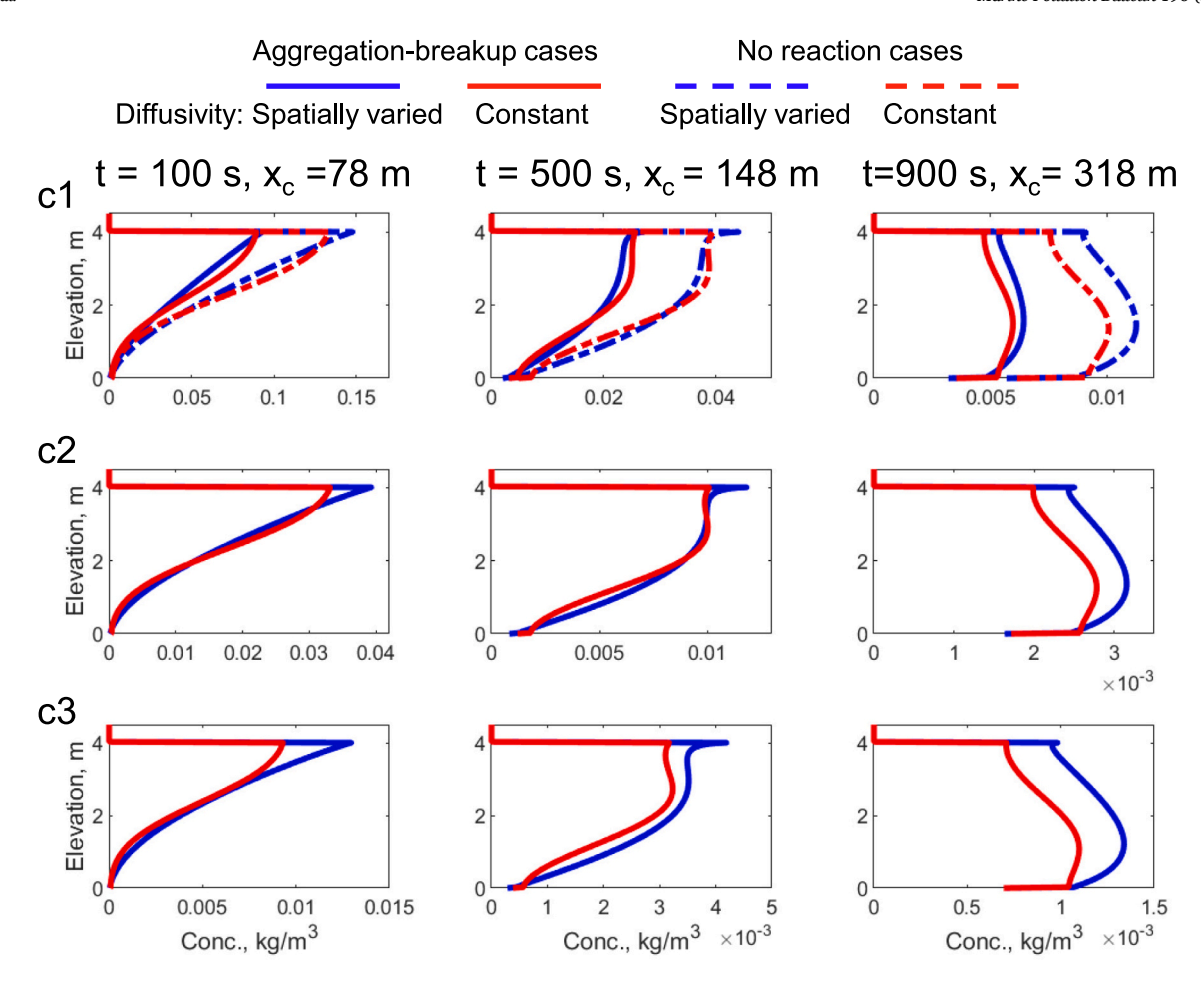


Fig. 5. Concentration distribution of microplastics within different size bins (c1-c3) along the vertical centerline of the microplastic plume for different simulated cases. Note that c1, c2, and c3 represent the first three size bins, respectively.

The aggregation and breakage process provides significant control on the particle size distribution of microplastics in river systems. Fig. 6a and b shows the concentration of different size particles at the center of the microplastic plume, simulated with spatially varied and constant diffusivity, respectively. The mass concentration decreased with time for the microplastics within all size bins, which is mainly due to the dispersion of the microplastic plume along its downstream path. Note that in the early time of t = 200 s and 400 s, due to less dispersion, the concentration is slightly higher at the center of the microplastic plume for the case simulated with the constant diffusivity. This is consistent with the results illustrated in Fig. 5. Compared to mass concentration, the volume fraction of different size microplastics tended to be stable after 200 s of the release for both the simulated cases (Fig. 6c and d). Only a slight change in volume fraction was observed afterward, indicating that significant aggregation of microplastics occurred in the early time of the release. This phenomenon can be interpreted by the underlying mechanism of particle aggregation, mathematically expressed in Eqs. (7)–(8). The extent of particle aggregation is related to particle population density (i.e., the number of particles per unit volume). A dense particle population of the microplastic plume at the initial stage of the release facilitated the aggregation of small-size particles into largersize aggregates. By contrast, after the release, the microplastic plume became more dispersed and diluted with time, and the subsequent low population density of the particles limited the aggregation process of microplastics in the river.

Aggregation and breakage are important processes when microplastics are released into a river system. The simulations conducted

herein show that a significant amount of microplastics aggregated into larger size particles after the release in the river (Fig. 7a). After the microplastics were released into the river, there was a sharp increase in the cumulative mass of the microplastics within large-size bins within the first 10 min, particularly for the particles within the size bins c2 and c3 (Fig. 7a). It indicates that at the early stage, a significant amount of the microplastics within the size bin c1 aggregated into larger size particles in the river. The increase in cumulative mass became slower at a later stage (t > 10 min). It is probably because as the microplastic aggregates accumulated in the river, the breakage of these aggregates came to be significant, which attenuated the mass accumulation of microplastics within the large-size bins. Our simulation results show that after an hour of the release, the mass of microplastics within the first five size bins (i.e., c1-c5) accounted for approximately 50 %, 30 %, 15 %, 4 %, and 1 % of the total mass, respectively (Fig. 7b). It indicates a significant change in the particle size distribution of the microplastics in the river after the initial release due to the aggregation-breakage process. Our simulation results also show a slight difference in predicting aggregation and breakage of microplastics in a river system when different spatial patterns of eddy diffusivity were adopted in the simulations. The case simulated with the constant eddy diffusivity resulted in a lower amount of microplastic aggregation in the river. For the case simulated with the constant diffusivity, the microplastic plume became more dispersed, and it consequently induced a lower population density of particles that to some extent limited the aggregation of particles in the river.

Particle concentration and energy dissipation rate are major

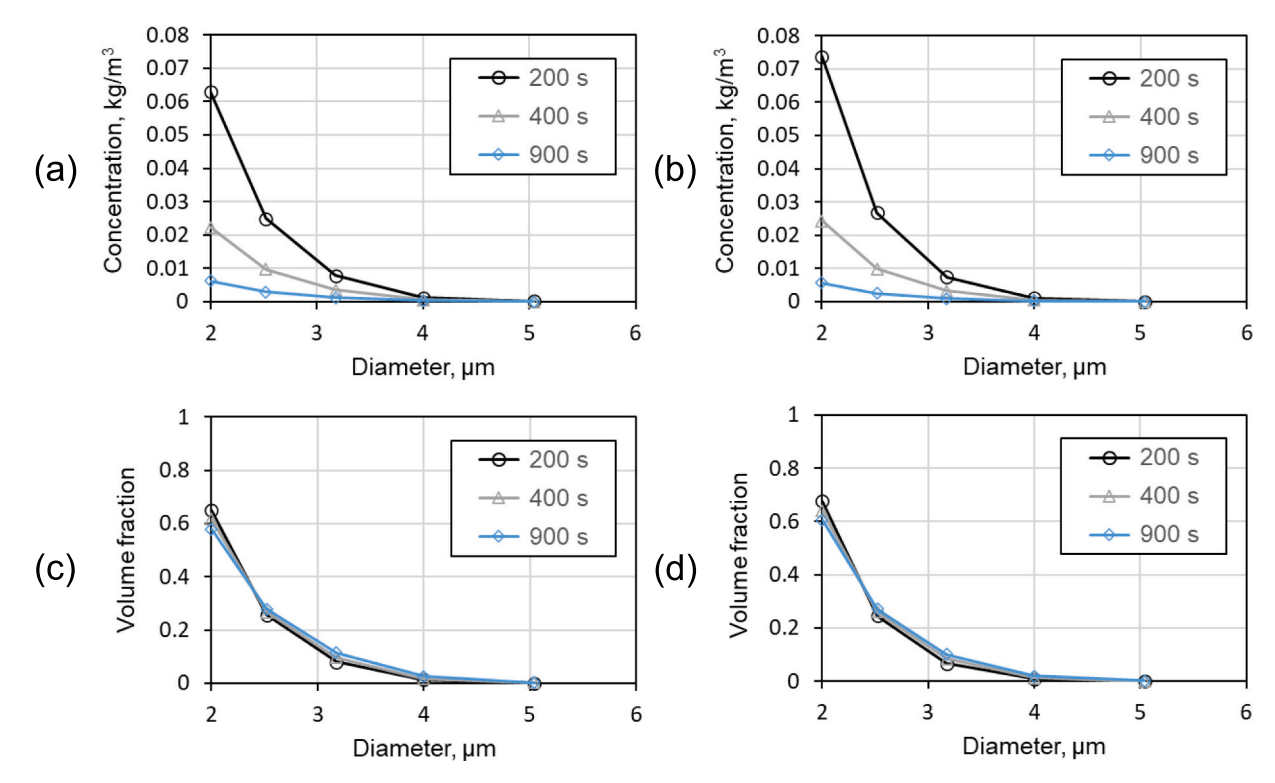


Fig. 6. (a-b) Mass concentration and (c-d) volume fraction of microplastics with different sizes for the simulated cases with spatially varied and constant eddy diffusivity, respectively.

controlling factors of the microplastic aggregation-breakage process in river systems. Fig. 8 shows the steady-state volume fraction of different size microplastics under different conditions of mass concentration and energy dissipation rate without considering river hydrodynamics. High particle concentration prompted the aggregation of microplastics. As shown in the figure, the steady-state volume fraction for large-size aggregates was remarkably elevated with an increase in particle concentration. In particular, for high-energy-dissipation cases (e.g., ϵ =1 \times 10^{-3} m²/s³ and 1×10^{-4} m²/s³), the peak size of particle aggregates increased from the initial size of 2 μm to over 100 μm when the particle concentration reached above 0.7 kg/m³. The energy dissipation rate also positively affected the microplastic aggregation process. As the energy dissipation rate increased from 1×10^{-6} m²/s³ to 1×10^{-5} m²/s³, and to 1×10^{-4} m²/s⁴, for the cases simulated with the largest concentration of 1 kg/m³, the peak size of the particle aggregates increased from 5 µm to 25 μ m, and to ~500 μ m, respectively. Interestingly, as the energy dissipation rate further increased from 1×10^{-4} m²/s³ to 1×10^{-3} m²/ s^3 , the peak size of the particles remained at ~500 µm, but its volume fraction decreased from 73 % to 55 %. This is most likely because the high energy dissipation rate also intensified the breakage of aggregates that to some extent attenuated the volume fraction of the largest-size aggregates. Our results also demonstrated that particle aggregation was significantly prohibited when the particle concentration and energy dissipation rate were both extremely low, particularly for the cases simulated with particle concentration <0.01 kg/m³ and energy dissipation rate lower than 1×10^{-3} m²/s³. It indicates that particle concentration and energy dissipation rate are equally important for particle aggregation to occur.

4. Discussion

This study highlights the importance of integrating various fundamental physical processes into simulations of the fate and transport of microplastics in riverine systems. Rivers provide important pathways for inland-produced microplastics to enter marine environments (Sarijan

et al., 2021; Su et al., 2022; van Wijnen et al., 2019). Thus, quantifying the fate and transport of microplastics in river systems is critical for sustainable management and risk assessment of plastic debris in terrestrial and aquatic environments (Er et al., 2023; Kumar et al., 2021; Tejaswini et al., 2022). Prior studies have revealed that rivers could create a dynamic hydraulic environment that strongly impacts the extent of aggregation and breakage of particles (e.g., oil droplets) at different downstream locations and depths of the river (Boufadel et al., 2019; Cui et al., 2021a; Cui et al., 2021b). Our simulation results revealed that river hydrodynamics significantly affected the aggregation and breakage processes of microplastics in rivers, and therefore, altered the particle size distribution of the microplastics within riverine systems. The primary driving factors of the aggregation-breakage process are particle concentration of microplastics and energy dissipation rate, and the interplay between these two factors results in a significantly distinct size distribution of microplastics within rivers. River-flowinduced transport (e.g., advection and dispersion) provides strong controls on tempo-spatial particle concentration distribution of microplastics in rivers, while river hydrodynamics determines the magnitude and distribution of energy dissipation rate along the river depth. Our findings indicate that transport dynamics have strong implications on the aggregation and breakage of microplastics in rivers. Meanwhile, aggregation and breakage of microplastics alter the buoyancy of the aggregates and thus affect the vertical transport process of microplastics in river systems. The strong interplay between the transport and aggregation-breakage process highlights a necessity to integrate multiple physical processes in simulating microplastic characteristics in rivers. Our results also identified the great extent of particle aggregation at the early stage of the release of microplastics in rivers, which is mainly caused by relatively high particle concentration after the initial release. It highlights the importance of understanding river hydrodynamics, especially near the source location, as well as the scale of microplastic pollution such as the amount and period of the release for more thorough assessing and mitigating microplastic pollution in the river environment.

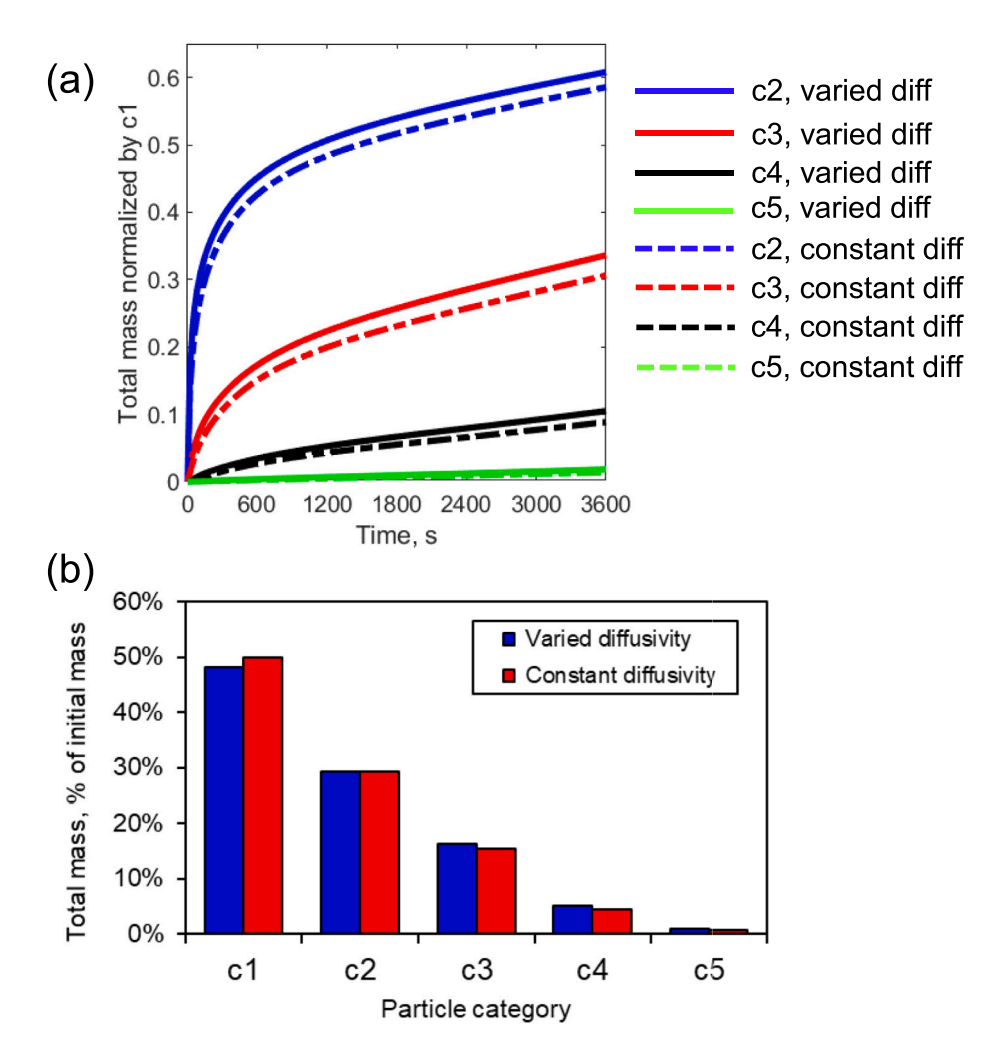


Fig. 7. (a) Temporal mass change and (b) the percentage mass distribution of the total mass after 1 h of the release for different size microplastics (c1–c5) that were simulated with spatially varied and constant eddy diffusivity, respectively. Note that c1, c2, c3, c4, and c5 represent the first five size bins, respectively.

In the paper, we considered the homo-aggregation of microplastics where aggregates are formed by microplastics among a range of particle sizes. Studies have revealed that microplastics in riverine environments also interact with other particles (e.g., phytoplankton) to form heteroaggregates that influences their downstream transport and distribution (Lagarde et al., 2016; Long et al., 2017; Yang et al., 2021). Microplastics might undergo other processes such as degradation and fragmentation (Andrady, 2017; Andrady and Koongolla, 2022; Sorasan et al., 2022), which are not considered in this paper. In addition, the aggregation behaviors of microplastics are influenced by other various factors, such as formation of biofilm, aggregating with other heavy particle (e.g., clay), zeta potentials, dissolved organic matters, and ionic strength. To gain a comprehensive understanding of the fate and transport of microplastics in rivers, future research should focus on modeling these processes, accompanied by proper model validation with real-world settings that integrate all the physical processes considered in the model. This work lays a sound foundation for such research.

5. Conclusion

In this paper, we developed a numerical modeling scheme using OpenFOAM to simulate the fate and transport of microplastics in a river system, taking into account various physical processes such as advection, dispersion, suspension, settling, aggregation, and breakage. This modeling scheme addresses the research gap in predicting the fate and

transport of microplastics in riverine systems by incorporating a range of physical driving mechanisms. Our simulation results show that microplastics experience significant aggregation and breakage when they transport downstream driven by river flows. It significantly alters the particle size distribution of microplastics in the river. The aggregationbreakage process of microplastics is primarily controlled by river hydrodynamics and pollution scale. Due to relatively high concentration, a great extent of particle aggregation occurs near the surface at the early stage of the release of microplastics in the river. At the later stage, the aggregation process becomes limited as the microplastic plume is gradually dispersed and diluted downstream. Due to the dispersion, strong aggregation of microplastics occurred at deep location due to relatively high energy dissipation rate close to the river bed. Eddy diffusivity drives the dispersion of the microplastic plume, and thus negatively affects the aggregation-breakage process of microplastics in the river. Overall, our numerical study demonstrates various physical processes that likely affect the fate and transport of microplastics in riverine systems. It highlights the importance of integrating various fundamental physical processes into simulations of the fate and transport of microplastics in riverine systems. The numerical modeling scheme established in this paper provides insights into the assessment and mitigation of microplastic pollution in river environments, which has the potential to be improved by incorporating additional processes as modules to further simulate the fate and transport of microplastics in more complex riverine environment.

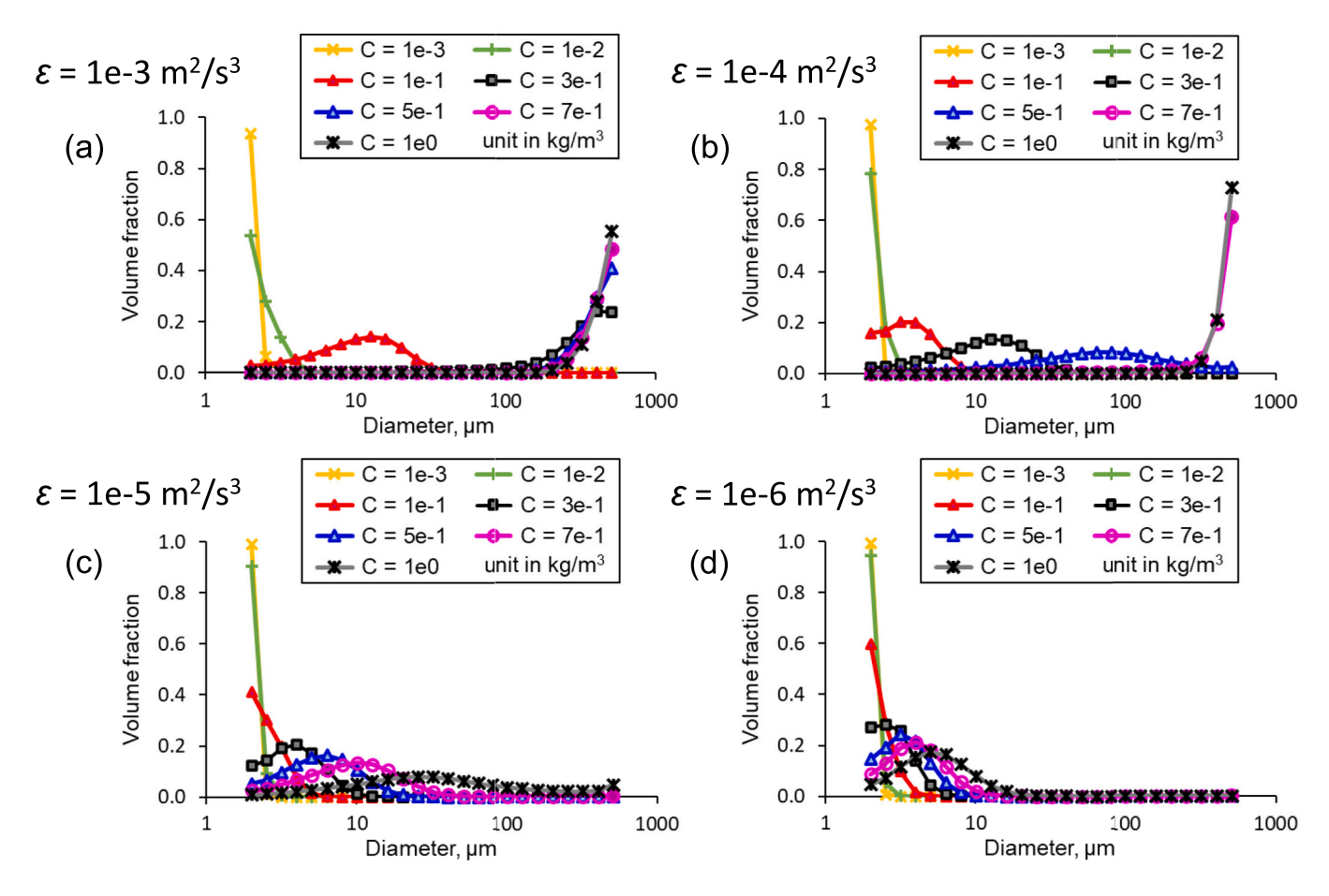


Fig. 8. (a-d) Steady-state volume fraction of different size microplastics for the cases simulated with different initial mass concentrations by using energy dissipation rate equal to 1×10^{-3} m²/s³, 1×10^{-4} m²/s³, 1×10^{-5} m²/s³, and 1×10^{-6} m²/s³, respectively. The initial mass concentration is labeled as C in the figure.

CRediT authorship contribution statement

Xiaolong Geng: Model Development, Methodology, Writing-Original draft preparation, and Numerical Simulations. Michel C. Boufadel: Conceptualization, Investigation, and Writing-Reviewing and Editing. Edward P. Lopez: Literature Review and Data Processing.

Declaration of competing interest

The authors declare that they have no known competing financial interests or personal relationships that could have appeared to influence the work reported in this paper.

Data availability

Data will be made available on request.

Acknowledgment

This work was funded by the US National Science Foundation (EAR2130595 and CBET2345629). However, it does not necessarily reflect the views of the funding agency, and no official endorsement should be inferred. This is SOEST contribution #11734.

References

Alimi, O.S., Farner Budarz, J., Hernandez, L.M., Tufenkji, N., 2018. Microplastics and nanoplastics in aquatic environments: aggregation, deposition, and enhanced contaminant transport. Environ. Sci. Technol. 52, 1704-1724.

Anbumani, S., Kakkar, P., 2018. Ecotoxicological effects of microplastics on biota: a review. Environ. Sci. Pollut. Res. 25, 14373-14396.

Andrady, A.L., 2017. The plastic in microplastics: a review. Mar. Pollut. Bull. 119, 12–22. Andrady, A.L., Koongolla, B., 2022. Degradation and fragmentation of microplastics. In: Plastics and the Ocean: Origin, Characterization, Fate, and Impacts, pp. 227-268.

Atugoda, T., Piyumali, H., Liyanage, S., Mahatantila, K., Vithanage, M., 2020. Fate and behavior of microplastics in freshwater systems. In: Handbook of Microplastics in the Environment, pp. 1–31.

Auta, H.S., Emenike, C., Fauziah, S., 2017. Distribution and importance of microplastics in the marine environment: a review of the sources, fate, effects, and potential solutions. Environ. Int. 102, 165-176.

Barton, L.E., Therezien, M., Auffan, M., Bottero, J.-Y., Wiesner, M.R., 2014. Theory and methodology for determining nanoparticle affinity for heteroaggregation in environmental matrices using batch measurements. Environ. Eng. Sci. 31, 421-427.

Borges-Ramírez, M.M., Mendoza-Franco, E.F., Escalona-Segura, G., Rendón-von Osten, J., 2020. Plastic density as a key factor in the presence of microplastic in the gastrointestinal tract of commercial fishes from Campeche Bay, Mexico. Environ. Pollut. 267, 115659.

Boufadel, M., Liu, R., Zhao, L., Lu, Y., Özgökmen, T., Nedwed, T., Lee, K., 2020. Transport of oil droplets in the upper ocean: impact of the eddy diffusivity. J. Geophys. Res. Oceans 125, e2019JC015727.

Boufadel, M.C., Cui, F., Katz, J., Nedwed, T., Lee, K., 2018. On the transport and modeling of dispersed oil under ice. Mar. Pollut. Bull. 135, 569-580.

Boufadel, M.C., Fitzpatrick, F., Cui, F., Lee, K., 2019. Computation of the mixing energy in rivers for oil dispersion. J. Environ. Eng. 145, 06019005.

Cao, R., Chen, H., Rong, Z., Lv, X., 2021. Impact of ocean waves on transport of underwater spilled oil in the Bohai Sea. Mar. Pollut. Bull. 171, 112702.

Chen, W., Fischer, R.R., Berg, J.C., 1990. Simulation of particle size distribution in an aggregation-breakup process, Chem. Eng. Sci. 45, 3003–3006.

Coles, D., 1956. The law of the wake in the turbulent boundary layer, J. Fluid Mech. 1, 191-226.

Coufort, C., Bouyer, D., Liné, A., Haut, B., 2007. Modelling of flocculation using a

population balance equation. Chem. Eng. Process. Process Intensif. 46, 1264–1273. Cui, F., Behzad, H., Geng, X., Zhao, L., Lee, K., Boufadel, M.C., 2021a. Dispersion of oil droplets in rivers. J. Hydraul. Eng. 147, 04021004. Cui, F., Daskiran, C., Lee, K., Boufadel, M.C., 2021b. Transport and formation of OPAs in

Rivers. J. Environ. Eng. 147, 04021012.

- Deng, Y., Zhang, Y., Lemos, B., Ren, H., 2017. Tissue accumulation of microplastics in mice and biomarker responses suggest widespread health risks of exposure. Sci. Rep. 7, 1–10
- Dris, R., Imhof, H., Sanchez, W., Gasperi, J., Galgani, F., Tassin, B., Laforsch, C., 2015. Beyond the ocean: contamination of freshwater ecosystems with (micro-) plastic particles. Environ. Chem. 12, 539–550.
- Dris, R., Gasperi, J., Mirande, C., Mandin, C., Guerrouache, M., Langlois, V., Tassin, B., 2017. A first overview of textile fibers, including microplastics, in indoor and outdoor environments. Environ. Pollut. 221, 453–458.
- Eo, S., Hong, S.H., Song, Y.K., Han, G.M., Shim, W.J., 2019. Spatiotemporal distribution and annual load of microplastics in the Nakdong River, South Korea. Water Res. 160, 228–237
- Er, C.T.X., Sen, L.Z., Srinophakun, P., Wei, O.C., 2023. Recent advances and challenges in sustainable management of plastic waste using biodegradation approach. Bioresour. Technol. 128772
- Eriksen, M., Maximenko, N., Thiel, M., Cummins, A., Lattin, G., Wilson, S., Hafner, J., Zellers, A., Rifman, S., 2013. Plastic pollution in the South Pacific subtropical gyre. Mar. Pollut. Bull. 68, 71–76.
- Ernest, A.N., Bonner, J.S., Autenrieth, R.L., 1995. Determination of particle collision efficiencies for flocculent transport models. J. Environ. Eng. 121, 320–329.
- Flesch, J.C., Spicer, P.T., Pratsinis, S.E., 1999. Laminar and turbulent shear-induced flocculation of fractal aggregates. AIChE J 45, 1114–1124.
- Gelbard, F., Tambour, Y., Seinfeld, J.H., 1980. Sectional representations for simulating aerosol dynamics. J. Colloid Interface Sci. 76, 541–556.
- Genc, A.N., Vural, N., Balas, L., 2020. Modeling transport of microplastics in enclosed coastal waters: a case study in the Fethiye Inner Bay. Mar. Pollut. Bull. 150, 110747.
- Geng, X., Boufadel, M.C., Lee, K., Abrams, S., Suidan, M., 2015. Biodegradation of subsurface oil in a tidally influenced sand beach: impact of hydraulics and interaction with pore water chemistry. Water Resour. Res. 51, 3193–3218.
- Geng, X., Pan, Z., Boufadel, M.C., Ozgokmen, T., Lee, K., Zhao, L., 2016. Simulation of oil bioremediation in a tidally influenced beach: spatiotemporal evolution of nutrient and dissolved oxygen. J. Geophys. Res. Oceans 121, 2385–2404.
- Geng, X., Boufadel, M.C., Cui, F., 2017. Numerical modeling of subsurface release and fate of benzene and toluene in coastal aquifers subjected to tides. J. Hydrol. 551, 793–803.
- Hinze, J.O., 1955. Fundamentals of the hydrodynamic mechanism of splitting in dispersion processes. AIChE J 1, 289–295.
- Hounslow, M., 1998. The population balance as a tool for understanding particle rate processes. Kona Powder Part. J. 16, 179–193.
- Hurley, R., Woodward, J., Rothwell, J.J., 2018. Microplastic contamination of river beds
- significantly reduced by catchment-wide flooding. Nat. Geosci. 11, 251–257.

 Ji, W., Boufadel, M., Zhao, L., Robinson, B., King, T., An, C., Zhang, B.H., Lee, K., 2021.

 Formation of oil-particle aggregates: impacts of mixing energy and duration. Sci.

 Total Environ. 795. 148781.
- Jiang, Q., Logan, B.E., 1991. Fractal dimensions of aggregates determined from steadystate size distributions. Environ. Sci. Technol. 25, 2031–2038.
- Kaku, V.J., Boufadel, M.C., Venosa, A.D., Weaver, J., 2006. Flow dynamics in eccentrically rotating flasks used for dispersant effectiveness testing. Environ. Fluid Mech. 6, 385–406.
- Khatmullina, L., Isachenko, I., 2017. Settling velocity of microplastic particles of regular shapes. Mar. Pollut. Bull. 114, 871–880.
- Koelmans, A.A., Bakir, A., Burton, G.A., Janssen, C.R., 2016. Microplastic as a vector for chemicals in the aquatic environment: critical review and model-supported reinterpretation of empirical studies. Environ. Sci. Technol. 50, 3315–3326.
- Komori, S., Murakami, Y., Ueda, H., 1989. The relationship between surface-renewal and bursting motions in an open-channel flow. J. Fluid Mech. 203, 103–123.
- Kooi, M., Besseling, E., Kroeze, C., Van Wezel, A.P., Koelmans, A.A., 2018. Modeling the fate and transport of plastic debris in freshwaters: review and guidance. In: Freshwater Microplastics, pp. 125–152.
- Kumar, R., Verma, A., Shome, A., Sinha, R., Sinha, S., Jha, P.K., Kumar, R., Kumar, P., Das, S., Sharma, P., 2021. Impacts of plastic pollution on ecosystem services, sustainable development goals, and need to focus on circular economy and policy interventions. Sustainability 13, 9963.
- Lagarde, F., Olivier, O., Zanella, M., Daniel, P., Hiard, S., Caruso, A., 2016. Microplastic interactions with freshwater microalgae: hetero-aggregation and changes in plastic density appear strongly dependent on polymer type. Environ. Pollut. 215, 331–339.
- Laist, D.W., 1997. Impacts of marine debris: entanglement of marine life in marine debris including a comprehensive list of species with entanglement and ingestion records. In: Marine Debris. Springer, pp. 99–139.
- Law, K.L., Thompson, R.C., 2014. Microplastics in the seas. Science 345, 144–145.
- Lebreton, L.C., Van Der Zwet, J., Damsteeg, J.-W., Slat, B., Andrady, A., Reisser, J., 2017. River plastic emissions to the world's oceans. Nat. Commun. 8, 1–10.
- Lebreton, L.-M., Greer, S., Borrero, J.C., 2012. Numerical modelling of floating debris in the world's oceans. Mar. Pollut. Bull. 64, 653–661.
- Lenaker, P.L., Corsi, S.R., Mason, S.A., 2020. Spatial distribution of microplastics in surficial benthic sediment of Lake Michigan and Lake Erie. Environ. Sci. Technol. 55, 373–384.
- Li, X.-y., Zhang, J.-j, 2003. Numerical simulation and experimental verification of particle coagulation dynamics for a pulsed input. J. Colloid Interface Sci. 262, 149–161.
- Limerinos, J.T., 1970. Determination of the Manning Coefficient from Measured Bed Roughness in Natural Channels.
- Liu, R., Boufadel, M.C., Zhao, L., Nedwed, T., Lee, K., Marcotte, G., Barker, C., 2022. Oil droplet formation and vertical transport in the upper ocean. Mar. Pollut. Bull. 176, 113451.

- Liu, R., Ji, W., Lee, K., Boufadel, M., 2023. Modeling the breakup of oil-particle aggregates in turbulent environments for projectile penetration. Langmuir. 39, 2808–2817.
- Long, M., Paul-Pont, I., Hegaret, H., Moriceau, B., Lambert, C., Huvet, A., Soudant, P., 2017. Interactions between polystyrene microplastics and marine phytoplankton lead to species-specific hetero-aggregation. Environ. Pollut. 228, 454–463.
- López, F., García, M., 1998. Open-channel flow through simulated vegetation: suspended sediment transport modeling. Water Resour. Res. 34, 2341–2352.
- Mai, L., You, S.-N., He, H., Bao, L.-J., Liu, L.-Y., Zeng, E.Y., 2019. Riverine microplastic pollution in the Pearl River Delta, China: are modeled estimates accurate? Environ. Sci. Technol. 53, 11810–11817.
- Mani, T., Hauk, A., Walter, U., Burkhardt-Holm, P., 2015. Microplastics profile along the Rhine River. Sci. Rep. 5, 1–7.
- McCormick, A.R., Hoellein, T.J., London, M.G., Hittie, J., Scott, J.W., Kelly, J.J., 2016. Microplastic in surface waters of urban rivers: concentration, sources, and associated bacterial assemblages. Ecosphere 7, e01556.
- Moore, C., Lattin, G., Zellers, A., 2005. Working our way upstream: a snapshot of land based contributions of plastic and other trash to coastal waters and beaches of Southern California. In: Proceedings of the Plastic Debris Rivers to Sea Conference, Algalita Marine Research Foundation, Long Beach, California. Citeseer.
- Mountford, A., Morales Maqueda, M., 2019. Eulerian modeling of the three-dimensional distribution of seven popular microplastic types in the global ocean. J. Geophys. Res. Oceans 124, 8558–8573.
- Nezu, I., 1977. Turbulent Structure in Open-channel Flows. Kyoto Univ, Kyoto, Japan. Nezu, I., 2005. Open-channel flow turbulence and its research prospect in the 21st century. J. Hydraul. Eng. 131, 229–246.
- Nezu, I., Nakagawa, H., 1993. Turbulence in Open-channel Flows, IAHR Monograph Series. AA Balkema, Rotterdam, Netherlands, pp. 1–281.
- Nezu, I., Nakagawa, H., Jirka, G.H., 1994. Turbulence in open-channel flows. J. Hydraul. Eng. 120, 1235–1237.
- NOAA National Ocean Service, 2016. What Are Microplastics? US Department of Commerce, National Oceanic and Atmospheric Administration.
- Pan, Z., Guo, H., Chen, H., Wang, S., Sun, X., Zou, Q., Zhang, Y., Lin, H., Cai, S., Huang, J., 2019. Microplastics in the Northwestern Pacific: abundance, distribution, and characteristics. Sci. Total Environ. 650, 1913–1922.
- Peng, S., Williams, R.A., 1994. Direct measurement of floc breakage in flowing suspensions. J. Colloid Interface Sci. 166, 321–332.
- PlasticsEurope, 2021. Plastics—the Facts 2021: an analysis of European plastics production, demand and waste data. In: PlasticsEurope AISBL Rue Belliard, 40 (b. (Ed.), Brussels, Belgium).
- Potemra, J.T., 2012. Numerical modeling with application to tracking marine debris.

 Mar. Pollut. Bull. 65, 42–50.
- Rillig, M.C., 2012. Microplastic in Terrestrial Ecosystems and the Soil? ACS Publications. Sarijan, S., Azman, S., Said, M.I.M., Jamal, M.H., 2021. Microplastics in freshwater ecosystems: a recent review of occurrence, analysis, potential impacts, and research needs. Environ. Sci. Pollut. Res. 28, 1341–1356.
- Schirinzi, G.F., Pérez-Pomeda, I., Sanchís, J., Rossini, C., Farré, M., Barceló, D., 2017. Cytotoxic effects of commonly used nanomaterials and microplastics on cerebral and epithelial human cells. Environ. Res. 159, 579–587.
- Seinfeld, J., Pandis, S., 2008. Atmospheric Chemistry and Physics (1997. New York). Shi, Z., Zhang, G., Zhang, Y., He, T., Pei, G., 2019. Modeling of flocculation and
- sedimentation using population balance equation. J. Chem. 2019. Siegfried, M., Koelmans, A.A., Besseling, E., Kroeze, C., 2017. Export of microplastics
- from land to sea. A modelling approach. Water Res. 127, 249–257. Smoluchowski, M.v., 1918. Versuch einer mathematischen Theorie der
- Koagulationskinetik kolloider Lösungen. Z. Phys. Chem. 92U, 129–168. Sorasan, C., Edo, C., González-Pleiter, M., Fernández-Piñas, F., Leganés, F.,
- Rodríguez, A., Rosal, R., 2022. Ageing and fragmentation of marine microplastics. Sci. Total Environ. 827, 154438.
- Su, L., Xiong, X., Zhang, Y., Wu, C., Xu, X., Sun, C., Shi, H., 2022. Global transportation of plastics and microplastics: a critical review of pathways and influences. Sci. Total Environ. 154884.
- Sutton, R., Mason, S.A., Stanek, S.K., Willis-Norton, E., Wren, I.F., Box, C., 2016. Microplastic contamination in the San Francisco Bay, California, USA. Mar. Pollut. Bull. 109, 230–235.
- Tejaswini, M., Pathak, P., Ramkrishna, S., Ganesh, S.P., 2022. A comprehensive review on integrative approach for sustainable management of plastic waste and its associated externalities. Sci. Total Environ. 153973.
- Terray, E.A., Donelan, M., Agrawal, Y., Drennan, W., Kahma, K., Williams, A.J., Hwang, P., Kitaigorodskii, S., 1996. Estimates of kinetic energy dissipation under breaking waves. J. Phys. Oceanogr. 26, 792–807.
- Tibbetts, J., Krause, S., Lynch, I., Sambrook Smith, G.H., 2018. Abundance, distribution, and drivers of microplastic contamination in urban river environments. Water 10, 1597.
- van der Wal, M., van der Meulen, M., Tweehuijsen, G., Peterlin, M., Palatinus, A., Kovac Viršek, M., 2015. SFRA0025: Identification and Assessment of Riverine Input of (Marine) Litter. Report for Michail Papadoyannakis, 186. DG Environment, United Kingdom.
- van Wijnen, J., Ragas, A.M., Kroeze, C., 2019. Modelling global river export of microplastics to the marine environment: sources and future trends. Sci. Total Environ. 673, 392–401.
- Vörösmarty, C., Fekete, B.M., Meybeck, M., Lammers, R.B., 2000. Global system of rivers: its role in organizing continental land mass and defining land-to-ocean linkages. Glob. Biogeochem. Cycles 14, 599–621.
- Wagner, M., Lambert, S., 2018. Freshwater Microplastics: Emerging Environmental Contaminants? Springer Nature.

- Waldschläger, K., Schüttrumpf, H., 2019. Effects of particle properties on the settling and rise velocities of microplastics in freshwater under laboratory conditions. Environ. Sci. Technol. 53, 1958–1966.
- White, F.M., 1991. Viscous fluid flow, mcgraw hill book company. N. Y. 19, 400.
- Williams, A., Simmons, S., 1996. The degradation of plastic litter in rivers: implications for beaches. J. Coast. Conserv. 2, 63–72.
- Wilson, T.P., Homologs Dec, P., 2006. Results of Cross-channel Monitoring During the Lower Passaic River Environmental Dredging Pilot Program on the Lower Passaic River, December 1 to 12, 2005. USGS Report, West Trenton, New Jersey (Page intentionally left blank).
- Yan, M., Wang, L., Dai, Y., Sun, H., Liu, C., 2021. Behavior of microplastics in inland waters: aggregation, settlement, and transport. Bull. Environ. Contam. Toxicol. 1–10.
- Yang, H., Chen, G., Wang, J., 2021. Microplastics in the marine environment: sources, fates, impacts and microbial degradation. Toxics 9, 41.
- Ye, L., Manning, A.J., Hsu, T.-J., 2020. Oil-mineral flocculation and settling velocity in saline water. Water Res. 173, 115569.
- Yonkos, L.T., Friedel, E.A., Perez-Reyes, A.C., Ghosal, S., Arthur, C.D., 2014.
 Microplastics in four estuarine rivers in the Chesapeake Bay, USA. Environ. Sci. Technol. 48, 14195–14202.

- Zhang, J.j., Li, X.y., 2003. Modeling particle-size distribution dynamics in a flocculation system. AIChE J 49, 1870–1882.
- Zhang, Z., Wu, H., Peng, G., Xu, P., Li, D., 2020. Coastal ocean dynamics reduce the export of microplastics to the open ocean. Sci. Total Environ. 713, 136634.
- Zhao, L., Torlapati, J., Boufadel, M.C., King, T., Robinson, B., Lee, K., 2014. VDROP: a comprehensive model for droplet formation of oils and gases in liquids-incorporation of the interfacial tension and droplet viscosity. Chem. Eng. J. 253, 93–106.
- Zhao, L., Boufadel, M.C., Adams, E., Socolofsky, S.A., King, T., Lee, K., Nedwed, T., 2015.
 Simulation of scenarios of oil droplet formation from the Deepwater Horizon blowout. Mar. Pollut. Bull. 101, 304–319.
- Zhao, L., Boufadel, M.C., Geng, X., Lee, K., King, T., Robinson, B., Fitzpatrick, F., 2016a. A-DROP: a predictive model for the formation of oil particle aggregates (OPAs). Mar. Pollut. Bull. 106, 245–259.
- Zhao, L., Wang, B., Armenante, P.M., Conmy, R., Boufadel, M.C., 2016b.
 Characterization of turbulent properties in the EPA baffled flask for dispersion effectiveness testing. J. Environ. Eng. 142, 04015044.
- Zhao, L., Boufadel, M.C., King, T., Robinson, B., Gao, F., Socolofsky, S.A., Lee, K., 2017. Droplet and bubble formation of combined oil and gas releases in subsea blowouts. Mar. Pollut. Bull. 120, 203–216.